

CYCLIC BEHAVIOUR OF REINFORCED CONCRETE COLUMNS  
INTERNALLY CONFINED BY CARBON FIBRE REINFORCED POLYMER  
STRIPS

NUR HAJARUL FALAH BINTI ABDUL HALIM

A thesis submitted in fulfilment of the  
requirements for the award of the degree of  
Doctor of Philosophy

School of Civil Engineering  
Faculty of Engineering  
Universiti Teknologi Malaysia

JANUARY 2020

## DEDICATION

**This thesis is dedicated to ummah, parents and husband**

"Indeed, Allah will not *change* the condition of a people until they *change* what is in themselves." -*Qur'an* (13:11)

"The best of people are those that bring most benefit to the rest of mankind."  
[Daraqutni, *Hasan*]

**Also, to my supervisors**

Assoc. Prof. Dr. Sophia C. Alih and Assoc. Prof. Dr. Mohamadreza Vafaei

Thanks for all the support, guidance and assistance throughout the whole thesis

## **ACKNOWLEDGEMENT**

Praise to God almighty, the compassionate and the merciful, who has created mankind with wisdom and given them knowledge.

Firstly, I would like to thank my supervisor and advisor, Assoc. Prof. Dr. Sophia C. Alih for her kind encouragement, earnest guidance, appreciative advices and friendly motivations. I also wish to thank my co-supervisor, Assoc. Prof. Dr. Mohammadreza Vafaei, for his grateful advices and impetus. Without continuous support from my supervisor and co-supervisor, this research would not be the same as presented in this thesis.

Secondly, I would like to thank the Dean, Head of structure and materials department, all lecturers and staff of the School of Civil Engineering UTM for the facilities provided by them that support and easier my path to do this research.

Last but not least, I want to express grateful thanks to my family, husband and friends for their infinity support and encouragement. Without their consistent support and encouragement, it was impossible for me to accomplish this work.

## ABSTRACT

Carbon fibre reinforced polymers (CFRP) sheets have been widely used in reinforced concrete (RC) structures for retrofitting. This study proposed the application of CFRP strips for internal confinement of RC columns. Experimental works, numerical simulations and analytical calculations were included in this study. Experimental works involved in quasi-static cyclic testing of eight full-scale RC columns that were internally confined by CFRP strips with different distances and widths. The specimens were divided into two groups a) column confined by CFRP stirrups (FRP) and b) column confined by CFRP spirals (SFRP). The obtained results from each group were compared with a reference column that was confined with the carbon steel bar. Numerical studies involved in a parametric investigation about the effects of different intensities of axial load and distances between CFRP strips on the cyclic responses of CFRP confined columns. Finite element models of two columns confined with CFRP stirrups and spirals were established in ABAQUS software and validated using the experimental results. Analytical calculations involved in proposing a step-by-step method for estimating the ultimate load of CFRP confined columns. The proposed method was verified through a comparison between experimental results and analytical calculations. Results of experimental works showed that all columns experienced a flexural type crack along their height. No buckling of longitudinal bars and CFRP rupture were observed. CFRP confined columns had up to 73% larger effective stiffness when compared with the reference columns. The CFRP confined columns also showed up to 63% larger ultimate load and effective yield strength when compared with the reference columns. Besides, the ductility ratio of CFRP confined columns was up to 48% larger than the reference columns. Moreover, the CFRP confined columns exhibited up to 96% larger cumulative energy dissipation and equivalent damping ratio when compared with the reference columns. Numerical simulation showed that the increase in the axial force of columns increased the stress on the surface of the concrete. The simulated columns showed buckling in longitudinal bars when the axial force was increased to 400 kN. Moreover, up to 45% reduction in the ultimate strength and its corresponding displacement were observed when axial force was increased to 400 kN. Increase in the axial force decreased the ductility ratio and effective yield strength of simulated columns up to 29%. Meanwhile, an increase in the distance between strips enlarged the area of the plastic zone in the concrete and longitudinal bars. Increase in the distance between CFRP strips decreased the ultimate load of columns up to 40%. The ductility ratio of columns was decreased by 22% when the distance between their strips was increased to 250 mm. Results also indicated that increase in the distance between strips decreased the effective yield strength of columns up to 35%. In summary, it was concluded that columns confined internally by CFRP stirrups and spirals had a superior cyclic behaviour when compared with the columns confined by carbon steel.

## ABSTRAK

Lembaran polimer bertetulang serat karbon (CFRP) telah digunakan secara meluas dalam struktur konkrit bertetulang (RC) untuk tujuan pengubahsuaian. Kajian ini mencadangkan penggunaan jalur CFRP untuk pelitupan dalaman tiang RC. Kerja-kerja eksperimen, simulasi berangka dan pengiraan analitik dimasukkan dalam kajian ini. Kerja-kerja eksperimen melibatkan ujian kitaran kuasi-statik terhadap lapan tiang RC berskala penuh yang dilitup secara dalaman oleh jalur CFRP dengan jarak dan lebar yang berlainan. Spesimen-spesimen dibahagikan kepada dua kumpulan a) tiang yang dilitup oleh jalur CFRP (FRP) dan b) tiang yang dilitup oleh lingkaran CFRP (SFRP). Keputusan yang diperoleh dari setiap kumpulan dibandingkan dengan tiang rujukan yang dilitupi dengan keluli karbon. Kajian berangka melibatkan penyiasatan parametrik mengenai kesan intensiti beban paksi yang berbeza dan jarak antara jalur CFRP dengan tindak balas kitaran bagi tiang yang dilitup oleh CFRP. Dua tiang model elemen terhingga yang dilitup dengan jalur dan lingkaran CFRP telah dibangunkan dalam perisian ABAQUS dan disahkan dengan menggunakan hasil eksperimen. Pengiraan analitik terlibat dalam mencadangkan kaedah langkah demi langkah untuk menganggar beban muktamad tiang yang dilitup oleh CFRP. Kaedah yang dicadangkan telah disahkan melalui perbandingan antara hasil eksperimen dan pengiraan analitik. Hasil kerja eksperimen menunjukkan bahawa semua tiang mengalami retakan jenis lentur sepanjang ketinggian. Tiada tetulang yang bengkok dan CFRP yang pecah dapat diperhatikan. Tiang yang terlitup oleh CFRP mempunyai kekukuhan berkesan 73% lebih besar jika dibandingkan dengan tiang rujukan. Tiang terlitup oleh CFRP juga menunjukkan kekuatan muatan tertinggi dan kekuatan muatan berkesan 63% lebih besar berbanding dengan tiang rujukan. Di samping itu, nisbah kemuluran tiang yang dilitup oleh CFRP adalah sehingga 48% lebih besar daripada tiang rujukan. Selain itu, tiang-tiang terlitup oleh CFRP mempamerkan pelepasan tenaga kumulatif dan nisbah redaman setara sehingga 96% lebih besar apabila dibandingkan dengan tiang rujukan. Simulasi berangka menunjukkan bahawa peningkatan kekuatan paksi tiang meningkatkan tekanan pada permukaan konkrit. Tiang simulasi menunjukkan tetulang membengkok apabila daya paksi dinaikkan kepada 400 kN. Selain itu, pengurangan sehingga 45% kekuatan muktamad dan jarak lenturan dapat diperhatikan apabila daya paksi dinaikkan kepada 400 kN. Peningkatan daya paksi didapati menurunkan nisbah kemuluran dan kekuatan efektif tiang simulasi maksimum sebanyak 29%. Sementara itu, peningkatan jarak antara jalur meningkatkan pembesaran kawasan zon plastik dalam konkrit dan tetulang. Peningkatan jarak antara jalur CFRP mengurangkan beban muktamad tiang sehingga 40%. Nisbah kemuluran tiang pula berkurang sebanyak 22% apabila jarak antara jalurnya meningkat kepada 250 mm. Hasil analisa juga menunjukkan bahawa peningkatan jarak antara jalur menurunkan kekuatan muatan berkesan tiang sehingga 35%. Ringkasnya, boleh disimpulkan bahawa tiang yang dilitup secara dalaman oleh jalur dan lingkaran CFRP mempunyai kelakuan kitaran yang tinggi apabila dibandingkan dengan tiang yang dikurungi oleh keluli karbon.

## TABLE OF CONTENTS

	<b>TITLE</b>	<b>PAGE</b>
	<b>DECLARATION</b>	<b>iii</b>
	<b>DEDICATION</b>	<b>iv</b>
	<b>ACKNOWLEDGEMENT</b>	<b>v</b>
	<b>ABSTRACT</b>	<b>vi</b>
	<b>ABSTRAK</b>	<b>vii</b>
	<b>TABLE OF CONTENTS</b>	<b>viii</b>
	<b>LIST OF TABLES</b>	<b>xiv</b>
	<b>LIST OF FIGURES</b>	<b>xvii</b>
	<b>LIST OF ABBREVIATIONS</b>	<b>xxviii</b>
	<b>LIST OF SYMBOLS</b>	<b>xxix</b>
	<b>LIST OF APPENDICES</b>	<b>xxxii</b>
<b>CHAPTER 1</b>	<b>INTRODUCTION</b>	<b>1</b>
1.1	Introduction	1
1.2	Problem Statement	3
1.3	Objective of Study	8
1.4	Scope of Study	9
1.5	Significance of Study	9
1.6	Outline of The Thesis	10
<b>CHAPTER 2</b>	<b>LITERATURE REVIEW</b>	<b>12</b>
2.1	Introduction	12
2.2	Failure Mechanism of RC Columns During Past Earthquake	14
2.3	Seismic Design Codes Requirement	22
2.3.1	American Concrete Institute (ACI)	22
2.3.1.1	Material Requirements	22
2.3.1.2	Detailing of Reinforcements	24

2.3.2	Eurocode 8 (2004) & Malaysia Standard (2017)	26
2.3.2.1	Material Requirements	27
2.3.2.2	Flexural and Shear Requirements	27
2.3.2.3	Detailing of Reinforcements	28
2.4	Effect of Stirrup Corrosion on the Performance of RC Structures	29
2.5	FRP Composites Reinforced Concrete Members	37
2.5.1	Externally Bonded FRPs	38
2.5.1.1	Column Tested Under Axial Load	38
2.5.1.2	Column Tested Under Cyclic Load	43
2.5.2	Reinforced Concrete Members Strengthened by FRP Bars	52
2.5.3	Application of FRPs in Real Structures	56
2.6	Durability of FRP Under Harsh Environment	59
2.6.1	Effects of Thermal Conditioning on FRPs	59
2.6.2	Effects of Chemical Solutions on FRPs	62
2.6.3	Effects of Hygrothermal Environment on FRPs	65
2.7	Usage of Other Reinforcing Materials	68
2.8	Summary	71
<b>CHAPTER 3</b>	<b>RESEARCH METHODOLOGY</b>	<b>74</b>
3.1	Introduction	74
3.2	Experimental Studies	75
3.2.1	Construction of Columns	80
3.2.2	Instrumentation and Test Setup	84
3.2.2.1	LVDTs	84
3.2.2.2	Strain Gauges	85
3.2.2.3	Load Cells	86
3.2.3	Test Setup of Specimens	87
3.3	Material Test	89

3.3.1	Concrete Test	89
3.3.2	Tensile Strength Test of Steel Rebars	91
3.3.3	Tensile Strength Test of CFRP	93
3.4	Finite Element Studies	94
3.4.1	Selection of Appropriate Software	94
3.4.2	Finite Element Modelling Approach	95
3.5	Analytical Study	103
3.5.1	Proposed Approach for the Calculation of Ultimate Load of CFRP Confined Columns	104
<b>CHAPTER 4</b>	<b>EXPERIMENTAL RESULTS AND ANALYSIS</b>	<b>109</b>
4.1	Introduction	109
4.2	Test Results of CSC Column	109
4.2.1	Failure Mechanism	109
4.2.2	Hysteresis Loops and Backbone Curve	111
4.2.3	Stiffness Degradation	114
4.2.4	Energy Dissipation	115
4.2.5	Strain Values	118
4.3	Test Results of FRP1 Column	121
4.3.1	Failure Mechanism	121
4.3.2	Hysteresis Loops and Backbone Curve	123
4.3.3	Stiffness Degradation	124
4.3.4	Energy Dissipation	125
4.3.5	Strain Values	127
4.4	Test Results of FRP2 Column	129
4.4.1	Failure Mechanism	130
4.4.2	Hysteresis Loops and Backbone Curve	131
4.4.3	Stiffness Degradation	133
4.4.4	Energy Dissipation	133
4.4.5	Strain Values	135
4.5	Test Results of FRP3 Column	137
4.5.1	Failure Mechanism	138
4.5.2	Hysteresis Loops and Backbone Curve	139



4.5.3	Stiffness Degradation	141
4.5.4	Energy Dissipation	141
4.5.5	Strain Values	143
4.6	Discussion on the Obtained Results of RC Columns Tested for the First Objective	146
4.7	Test Results of CSS Column	155
4.7.1	Failure Mechanism	155
4.7.2	Hysteresis Loops and Backbone Curve	156
4.7.3	Stiffness Degradation	158
4.7.4	Energy Dissipation	158
4.7.5	Strain Values	160
4.8	Test Results of SFRP1 Column	163
4.8.1	Failure Mechanism	163
4.8.2	Hysteresis Loops and Backbone Curve	165
4.8.3	Stiffness Degradation	166
4.8.4	Energy Dissipation	167
4.8.5	Strain Values	169
4.9	Test Results of SFRP2 Column	171
4.9.1	Failure Mechanism	172
4.9.2	Hysteresis Loops and Backbone Curve	173
4.9.3	Stiffness Degradation	175
4.9.4	Energy Dissipation	175
4.9.5	Strain Values	177
4.10	Test Results of SFRP3 Column	179
4.10.1	Failure Mechanism	180
4.10.2	Hysteresis Loops and Backbone Curve	181
4.10.3	Stiffness Degradation	183
4.10.4	Energy Dissipation	183
4.10.5	Strain Values	185
4.11	Discussion on the Obtained Results of RC Columns Tested for the Second Objective	188
4.12	Summary	196

<b>CHAPTER 5</b>	<b>NUMERICAL ANALYSIS</b>	<b>199</b>
5.1	Introduction	199
5.2	Calibration work of Finite Element Model	199
5.3	Validation of Finite Element Model	202
5.3.1	Comparison Between Force-Displacement Relationships	202
5.3.2	Comparison of Stress Distribution	203
5.3.3	Concluding Remark on the Validation of FE Models	205
5.4	Effects of Axial Force on Cyclic Behaviour of CFRP Confined Columns	206
5.4.1	Stress Distribution and Failure Mode of Columns	206
5.4.2	Ultimate Load and Corresponding Displacement	216
5.4.3	Effective Yield Strength and Ductility Ratio of Columns	220
5.4.4	Concluding Remark on the Effects of Axial Load	221
5.5	Effects of Larger Distance Between CFRP Strips	222
5.5.1	Stress Distribution and Failure Mode of Columns	222
5.5.2	Ultimate Load and Corresponding Displacement	231
5.5.3	Effective Yield Strength and Ductility Ratio of Columns	235
5.5.4	Concluding Remark on the Effects of Different Distances Between CFRP strips	236
5.6	Summary	237
<b>CHAPTER 6</b>	<b>ANALYTICAL STUDY</b>	<b>239</b>
6.1	Introduction	239
6.2	Validation of the Proposed Method	243
6.2.1	Calculation of Ultimate Load of FRP1 Column	240
6.2.2	Calculation of Ultimate Load of SFRP1 Column	244
6.4	Summary	248

<b>CHAPTER 7</b>	<b>CONCLUSION AND RECOMMENDATIONS</b>	<b>249</b>
7.1	Introduction	249
7.2	The Cyclic Response of RC Columns Confined by CFRP Strips	249
7.3	Effects of Different Intensities of Axial Force and Distances of CFRP strips on The Cyclic Response of CFRP Confined Columns	252
7.4	A Method for Estimating The Ultimate Load of CFRP Confined Column	253
7.5	Contribution to the Body Knowledge	254
7.6	Recommendation for Future Works	255
	<b>REFERENCES</b>	<b>256</b>
	<b>LIST OF PUBLICATIONS</b>	<b>277</b>

## LIST OF TABLES

TABLE NO.	TITLE	PAGE
Table 1.1	Summarised properties of FRP sheets and mild steel grade	8
Table 2.1	The summary of seismic-induced damage to RC buildings during post-earthquakes	20
Table 2.2	Limits for compressive strength of concrete, $f_c'$ according to ACI 318 (2014)	23
Table 2.3	Requirements for non-prestressed deformed reinforcement ACI 318 (2014)	23
Table 2.4	Requirements for non-prestressed plain spiral reinforcement ACI 318 (2014)	24
Table 2.5	Minimum inside bend diameters and standard hook geometry for stirrups, ties, and hoops according to ACI 318 (2014)	25
Table 2.6	Maximum spacing of shear reinforcement for column according to ACI 318 (2014)	26
Table 2.7	Specification of material requirements for medium and high ductile columns	27
Table 2.8	Studies on the effects of stirrups corrosion in RC elements	35
Table 2.9	Typical mechanical properties of FRPs (Günaslan <i>et al.</i> , 2014)	37
Table 2.10	Experimental details of axial test of columns confined with FRP sheets	42
Table 2.11	Studies on seismic behaviour of RC columns externally bonded FRP	49
Table 2.12	Properties of the longitudinal reinforcements of columns tested by Sun <i>et al.</i> (2017)	55
Table 2.13	Experimental study on FRP composites under elevated temperature	61
Table 2.14	Experimental studies on FRP composites in chemical solutions	65
Table 2.15	Experimental study of FRP composites in hygrothermal condition	68

Table 2.16	Comparison of mechanical properties of reinforcing bar alloys (McGurn, 1998)	69
Table 3.1	Types of laboratory specimens	77
Table 3.2	The mechanical properties of CFRP sheets given by manufacturer (MAPEI Malaysia, 2018)	82
Table 3.3	Compression test results of cubic samples	90
Table 3.4	Tensile strength test results for steel reinforcement bars	92
Table 3.5	Results obtained from the tensile strength test of CFRP strip	94
Table 3.6	Plastic damage parameters for CDP suggested by manual of ABAQUS (2014)	96
Table 3.7	Properties of cohesive contact (Sugiman <i>et al.</i> , 2013)	103
Table 4.1	Structural characteristics obtained from the idealised backbone curve of CSC column	114
Table 4.2	Structural characteristics obtained from the idealised backbone curve of FRP1 column	124
Table 4.3	Structural characteristics obtained from the idealised backbone curve of FRP2 column	132
Table 4.4	Structural characteristics obtained from the idealised backbone curve of FRP3 column	140
Table 4.5	Summary of obtained experimental results	154
Table 4.6	Structural characteristics obtained from the idealised backbone curve of CSS column	157
Table 4.7	Structural characteristics obtained from the idealised backbone curve of SFRP1 column	166
Table 4.8	Structural characteristics obtained from the idealised backbone curve of SFRP2 column	174
Table 4.9	Structural characteristics obtained from the idealised backbone curve of SFRP3 column	182
Table 4.10	Summary of obtained experimental results from push direction	194
Table 5.1	Comparison between initial stiffness, ultimate lateral load and its corresponding displacement	206
Table 5.2	Results obtained from the backbone curves of FRP1 column with different intensities of axial load	218

Table 5.3	Results obtained from the backbone curves of SFRP1 column with different intensities of axial load	220
Table 5.4	Comparison of the effective yield strength and ductility ratio of FRP1 columns with different intensities of axial load	221
Table 5.5	Comparison of effective yield strength and ductility ratio of SFRP1 columns with different intensities of axial load	221
Table 5.6	Results from backbone curves of FRP1 column with different distances between stirrups	233
Table 5.7	Results from backbone curves of SFRP1 column with different distances between spirals	235
Table 5.8	Comparison of effective yield strength and ductility ratio of FE models for FRP1 columns with different distances between CFRP stirrups	235
Table 5.9	Comparison of effective yield strength and ductility ratio of FE models for SFRP1 columns with different distances between CFRP stirrups	236
Table 6.1	Information of material properties used to calculate the ultimate load capacity of columns	240

## LIST OF FIGURES

FIGURE NO.	TITLE	PAGE
Figure 1.1	Columns failure in RC buildings due to poor shear design during 2004 Sumatra Earthquake and Tsunami; (a), (b) and (c) buckling of longitudinal bars due to 90° hooks opened up and (d) shear failure of column at beam-columns joint (Kaushik and Jain, 2007)	2
Figure 1.2	FRP sheets wrapped around RC parts to enhance shear and flexure strength; (a) columns and (b) garage beams (Alkhrdaji, 2015)	2
Figure 1.3	Typical stress-strain curves of confined and unconfined concrete (Mander <i>et al.</i> , 1988)	4
Figure 1.4	Corrosion damage of RC columns; (a) completely deteriorated of stirrups and (b) severe damage of steel rebars (Tapan <i>et al.</i> , 2016)	4
Figure 1.5	The compressive strength of (a) corroded core concrete and (b) corroded concrete cover (Yu <i>et al.</i> , 2020)	5
Figure 1.6	Large spacing between the stirrups lead to column failure; (a) damaged column during 2015 Gorkha Earthquake and (b) column failure lead to building collapses during 2004 Sumatra Earthquake and Tsunami (Saatcioglu <i>et al.</i> , 2005; Sharma <i>et al.</i> , 2016)	5
Figure 1.7	Buckling of longitudinal reinforcement during earthquakes due to improper detailing of confinement; (a) Expo building, Talcahuano during 2010 Chile Earthquake and Tsunami, (b) Van Nuys Holiday Inn building, California 1994 Northridge Earthquake, (c) Imperial County Services building California 1994 Northridge Earthquake and (d) Parking garage of the Digicel building 2010 Haiti earthquake (Olsen <i>et al.</i> , 2010; Faison <i>et al.</i> , 2004; Paultre <i>et al.</i> , 2013)	6
Figure 2.1	The overview of the literature review	13
Figure 2.2	Damage columns due to inadequate/poor detailing; (a) lack of transverse reinforcement in beam-column joints, (b) large spacing between the stirrups (Alih and Vafaei, 2019)	15
Figure 2.3	Poor detailing of stirrups; (a) corroded stirrups with 90° hook and (b) unwounded stirrups with short hook (Sharma <i>et al.</i> , 2016)	15

Figure 2.4	Damaged columns during 2011 Lorca earthquake: (a) shear failure and (b) plastic hinge at the top of the column (Ruiz-Pinilla <i>et al.</i> , 2016)	16
Figure 2.5	Collapse of “Casa dello Studente” building; (a) North view and (b) West view (Mulas <i>et al.</i> , 2013)	18
Figure 2.6	Transverse reinforcement detailing of columns for earthquake forces according to ACI 318 (2014)	26
Figure 2.7	Detailing of primary seismic RC columns according to Eurocode 8 (2004)	29
Figure 2.8	Example of corroded steel stirrup in RC columns (Tapan <i>et al.</i> , 2016)	33
Figure 2.9	Schematic diagram for test setup (Mooty <i>et al.</i> , 2006)	44
Figure 2.10	Different wrapping configuration employed for columns (Colomb <i>et al.</i> , 2008)	44
Figure 2.11	FRP arrangement samples tested by Ali <i>et al.</i> (2018): (a) FRP spirals and (b) FRP hoops	54
Figure 2.12	Use of FRP reinforcement in real structures; (a) CFRP grid of substructure, (b) Seismic retrofitting of tall piers (Kobayashi <i>et al.</i> , 2009), (c) Near-surface-mounted (NSM) FRP in the cantilevered portion of a bridge deck (Augenti <i>et al.</i> , 2013) and (d) Underwater repair using FRPs (Sen and Mullins, 2007)	57
Figure 2.13	SEM images of fractured surfaces (Grammatikos <i>et al.</i> , 2016)	67
Figure 3.1	Selected research methodology for this study	75
Figure 3.2	Constructed columns for the 1 <sup>st</sup> group: (a) reference column, (b) Column transversely reinforced by CFRP strip stirrups (15 mm width) at 100 mm, (c) Column transversely reinforced by CFRP strip stirrups (7.5 mm width, double thickness) at 100 mm distance and (d) Column transversely reinforced by CFRP strip stirrups (15 mm width) at 150 mm distance	78
Figure 3.3	Constructed columns for the 2 <sup>nd</sup> group: (a) reference column, (b) Column transversely reinforced by CFRP strip spirals (15 mm width) at 100 mm, (c) Column transversely reinforced by CFRP strip spirals (7.5 mm width, double thickness) at 100 mm distance and (d) Column transversely reinforced by CFRP strip spirals (15 mm width) at 150 mm distance	79
Figure 3.4	Details of footing: (a) plan and (b) section A-A	79



Figure 3.5	Construction of reinforcement cages for; (a) column with stirrup as the transverse reinforcement and (b) column with spiral as the transverse reinforcement	80
Figure 3.6	Construction of reinforcement cages for CFRP confined columns; (a) before wrapping of CFRP strips and (b) during the installation of CFRP strips	81
Figure 3.7	Prepared CFRP strips for wrapping of columns	82
Figure 3.8	Reinforcement cages with CFRP strips as transverse reinforcement; (a) CFRP strips in the form of stirrup (b) CFRP strips in the form of spiral	82
Figure 3.9	Concreting of the columns; a) reinforcement cage placed within the formwork and b) casting of samples	83
Figure 3.10	Curing of columns; a) samples covered with gunny sack and b) painted samples after curing was completed	84
Figure 3.11	Location of LVDTs	85
Figure 3.12	Installed strain gauges; (a) surface of concrete, (b) longitudinal steel bars and transverse reinforcements	86
Figure 3.13	Location of installed load cells	87
Figure 3.14	Employed test set up: (a) schematic diagram and (b) lab test	88
Figure 3.15	Loading protocol according to FEMA 461 (2007)	89
Figure 3.16	Compressive test of concrete cube; (a) testing machine and (b) tested cubic samples	90
Figure 3.17	Modulus of elasticity and Poisson's ratio: (a) testing machine and (b) tested cylinder	91
Figure 3.18	Tensile strength test of steel bars; (a) sample of steel bars and (b) tested steel bars	92
Figure 3.19	Stress-strain curves of three samples of steel reinforcement bars: (a) ribbed rebar with 12 mm diameter and (b) plain rebar with 6 mm diameter	92
Figure 3.20	Configuration of CFRP coupons	93
Figure 3.21	Failure mode of the tested CFRP strips	93
Figure 3.22	Geometry of selected elements in ABAQUS: (a) 8-node solid and (b) 2-node linear	97
Figure 3.23	Conventional versus continuum shell element	97
Figure 3.24	Stress-strain curves of concrete with 25MPa compressive	98

Figure 3.25	Stress-strain curves of reinforcement with 12 mm diameter	98
Figure 3.26	Effect of mesh size on lateral displacement as compared with laboratory results	99
Figure 3.27	Finite element model for concrete sections	100
Figure 3.28	Finite element model of reinforcements for columns internally confined with CFRP stirrup	100
Figure 3.29	Finite element model of reinforcements for columns internally confined with CFRP spirals	101
Figure 3.30	Contact surface between CFRP strips and steel bars	102
Figure 3.31	Boundary conditions of supports	103
Figure 3.32	Flowchart of the proposed method for the calculation of ultimate load of CFRP confined columns	107
Figure 3.33	Illustration of strain distribution for columns confined by CFRP strips: (a) CFRP stirrups and (b) CFRP spirals	108
Figure 4.1	Crack pattern along the height of the column: (a) front side, (b) back side, (c) left side and (d) right side	110
Figure 4.2	Concrete crushing and spalling at the base of column: (a) front side and (b) right side	111
Figure 4.3	Idealised force-displacement curve according to FEMA 356 (2000)	112
Figure 4.4	Hysteresis curve of CSC column	113
Figure 4.5	Backbone curve and its bilinear representation of CSC column	113
Figure 4.6	Stiffness degradation of CSC column	115
Figure 4.7	Calculation of (a) equivalent damping ratio (He <i>et al.</i> , 2016) and (b) relative energy dissipation (Mojarradbahreh and Elbadry, 2014)	116
Figure 4.8	Absolute energy dissipation of CSC column	117
Figure 4.9	Cumulative energy dissipation of CSC column	117
Figure 4.10	Relative energy dissipation of CSC column	117
Figure 4.11	Equivalent damping ratio of CSC column	118
Figure 4.12	Strain values measured on concrete surface of CSC column: (a) measured strain in horizontal direction at the base of the column and (b) measured strain in vertical direction at the base of the column	120

Figure 4.13	Strain values in longitudinal bars of CSC column	120
Figure 4.14	Strain values in transverse bars of CSC column	121
Figure 4.15	Crack pattern along the height of the column: (a) front side, (b) back side, (c) left side and (d) right side	122
Figure 4.16	(a) Concrete spalling at the base of the column and (b) exposure of reinforcement bars	122
Figure 4.17	Hysteresis loops of FRP1 column	123
Figure 4.18	Backbone curve and its bilinear representation of FRP1 column	124
Figure 4.19	Stiffness degradation of FRP1 column	125
Figure 4.20	Absolute energy dissipation of FRP1 column	126
Figure 4.21	Cumulative energy dissipation of FRP1 column	126
Figure 4.22	Relative energy dissipation of FRP1 column	126
Figure 4.23	Equivalent damping ratio of FRP1 column	127
Figure 4.24	Strain values measured on concrete surface of FRP1 column: (a) measured strain in horizontal direction at the base of the column and (b) measured strain in vertical direction at the base of the column	128
Figure 4.25	Strain distribution in longitudinal bars of FRP1 column	129
Figure 4.26	Strain distribution in transverse bar of FRP1 column	129
Figure 4.27	Crack pattern along the height of the column: (a) front side, (b) back side, (c) left side and (d) right side	130
Figure 4.28	(a) Concrete spalling at the base of the column and (b) exposure of reinforcement bars	131
Figure 4.29	Hysteresis loops of FRP2 column	132
Figure 4.30	Backbone curve and its bilinear representation of FRP2 column	132
Figure 4.31	Stiffness degradation of FRP2 column	133
Figure 4.32	Absolute energy dissipation of FRP2 column	134
Figure 4.33	Cumulative energy dissipation of FRP2 column	134
Figure 4.34	Relative energy dissipation of FRP2 column	134
Figure 4.35	Equivalent damping ratio of FRP2 column	135
Figure 4.36	Strain values measured on concrete surface of FRP2 column: (a) measured strain in horizontal direction at the	

	base of the column and (b) measured strain in vertical direction at the base of the column	136
Figure 4.37	Strain distribution in longitudinal bars of FRP2 column	137
Figure 4.38	Strain distribution in transverse bar of FRP2 column	137
Figure 4.39	Crack pattern along the height of the column: (a) front side, (b) back side, (c) left side and (d) right side	138
Figure 4.40	(a) Large cracks at the base of the column and b) exposure of reinforcement bars	139
Figure 4.41	Hysteresis loops of FRP3 column	140
Figure 4.42	Backbone curve and its bilinear representation of FRP3 column	140
Figure 4.43	Stiffness degradation of FRP3 column	141
Figure 4.44	Absolute energy dissipation of FRP3 column	142
Figure 4.45	Cumulative energy dissipation of FRP3 column	142
Figure 4.46	Relative energy dissipation of FRP3 column	143
Figure 4.47	Equivalent damping ratio of FRP3 column	143
Figure 4.48	Strain values on concrete surface of FRP3 column: (a) measured strain in horizontal direction at the base of the column and (b) measured strain in vertical direction at the base of the column	145
Figure 4.49	Strain distribution in longitudinal bars of FRP3 column	145
Figure 4.50	Strain distribution in transverse bar of FRP3 column	146
Figure 4.51	Comparison of the observed crack patterns for front view of columns: (a) CSC, (b) FRP1, (c) FRP2 and (d) FRP3	147
Figure 4.52	Comparison of hysteresis curves of all columns tested for the 1 <sup>st</sup> group	149
Figure 4.53	Comparison of backbone curves of all columns tested for the 1 <sup>st</sup> group	149
Figure 4.54	Comparison of stiffness degradation of all columns tested for the 1 <sup>st</sup> group	150
Figure 4.55	Comparison of cumulative energy dissipation capacity of all columns tested for the 1 <sup>st</sup> group	152
Figure 4.56	Cracks pattern along the height of the column: (a) front side, (b) back side, (c) left side and (d) right side	155

Figure 4.57	Concrete crushing and spalling at the base of the column; a) front view and b) side view	156
Figure 4.58	Hysteresis loops of CSS column	157
Figure 4.59	Backbone curve and its bilinear representation of CSS column	157
Figure 4.60	Stiffness degradation of CSS column	158
Figure 4.61	Absolute energy dissipation of CSS column	159
Figure 4.62	Cumulative energy dissipation of CSS column	159
Figure 4.63	Relative energy dissipation of CSS column	160
Figure 4.64	Equivalent damping ratio of CSS column	160
Figure 4.65	Strain values measured on concrete surface of CSS column: (a) measured strain in horizontal direction at the base of the column and (b) measured strain in vertical direction at the base of the column	162
Figure 4.66	Strain distribution in longitudinal bars of CSS column	162
Figure 4.67	Strain distribution in transverse bars of CSS column	163
Figure 4.68	Crack pattern along the height of the column: (a) front side, (b) back side, (c) left side and (d) right side	164
Figure 4.69	(a) Concrete spalling at the base of the column and (b) exposure of reinforcement bar	164
Figure 4.70	Hysteresis loops of SFRP1 column	165
Figure 4.71	Backbone curve and its bilinear representation of SFRP1 column	166
Figure 4.72	Stiffness degradation of SFRP1 column	167
Figure 4.73	Absolute energy dissipation of SFRP1 column	168
Figure 4.74	Cumulative energy dissipation of SFRP1 column	168
Figure 4.75	Relative energy dissipation of SFRP1 column	168
Figure 4.76	Equivalent damping ratio of SFRP1 column	169
Figure 4.77	Strain values on concrete surface of SFRP1 column: (a) measured strain in horizontal direction at the base of the column and (b) measured strain in vertical direction at the base of the column	170
Figure 4.78	Strain distribution in longitudinal bars of SFRP1 column	171
Figure 4.79	Strain distribution in transverse bar of SFRP1 column	171

Figure 4.80	Crack pattern along the height of the column: (a) front side, (b) back side, (c) left side and (d) right side	172
Figure 4.81	(a) Concrete crushing at the corner of the column and b) exposure of reinforcement bars	174
Figure 4.82	Hysteresis loops of SFRP2 column	175
Figure 4.83	Backbone curve and its bilinear representation of SFRP2 column	175
Figure 4.84	Stiffness degradation of SFRP2 column	176
Figure 4.85	Absolute energy dissipation of SFRP2 column	177
Figure 4.86	Cumulative energy dissipation of SFRP2 column	177
Figure 4.87	Relative energy dissipation of SFRP2 column	177
Figure 4.88	Equivalent damping ratio of SFRP2 column	178
Figure 4.89	Strain values on concrete surface of SFRP2 column: (a) measured strain in horizontal direction at the base of the column and (b) measured strain in vertical direction at the base of the column	179
Figure 4.90	Strain distribution in longitudinal bars of SFRP2 column	180
Figure 4.91	Strain distribution in transverse bar of SFRP2 column	180
Figure 4.92	Crack pattern along the height of the column: (a) front side, (b) back side, (c) left side and (d) right side	181
Figure 4.93	(a) Concrete crushing and spalling and (b) exposure of reinforcement bars	182
Figure 4.94	Hysteresis loops of SFRP3 column	183
Figure 4.95	Backbone curve and its bilinear representation of SFRP3 column	183
Figure 4.96	Stiffness degradation of SFRP3 column	184
Figure 4.97	Absolute energy dissipation of SFRP3 column	185
Figure 4.98	Cumulative energy dissipation of SFRP3 column	185
Figure 4.99	Relative energy dissipation of SFRP3 column	186
Figure 4.100	Equivalent damping ratio of SFRP3 column	186
Figure 4.101	Strain values on concrete surface of SFRP3 column: (a) measured strain in horizontal direction at the base of the column and (b) measured strain in vertical direction at the base of the column	187

Figure 4.102	Strain distribution in longitudinal bars of SFRP3 column	187
Figure 4.103	Strain distribution in transverse bar of SFRP3 column	188
Figure 4.104	Comparison of the observed crack patterns for front view of columns: (a) CSS, (b) SFRP1, (c) SFRP2 and (d) SFRP3	189
Figure 4.105	Comparison of hysteresis curves of all columns tested for the 2nd group	191
Figure 4.106	Comparison of backbone curves of all columns tested for the 2nd group	191
Figure 4.107	Comparison of stiffness degradation of all columns tested for the 2nd group	192
Figure 4.108	Comparison of cumulative energy dissipation capacity of all columns tested for the 2nd group	194
Figure 5.1	Geometrical properties of RC column according to Vahed, (2017)	200
Figure 5.2	Results obtained from FE model: (a) hysteresis curve and (b) comparisons of backbone curves between FEM and experiment	201
Figure 5.3	Cracking and failure mode of the RC column; (a) Experimental works (Vahed, 2017) and (b) FE model	201
Figure 5.4	Comparison between force-displacement relationship of FE model and experimental test of FRP1 column	203
Figure 5.5	Comparison between force-displacement relationship of FE model and experimental test of SFRP1 column	203
Figure 5.6	Comparison of stress distribution for FRP1 column: (a) left side of column and (b) bottom of column	204
Figure 5.7	Comparison of stress distribution for SFRP1 column: (a) left side of column and (b) bottom of column	205
Figure 5.8	The force-stress curves on the concrete surface of FRP1 column for different axial load intensities	208
Figure 5.9	Stress distributions on the concrete surface of FRP1 column at 5% drift: (a) 70 kN, (b)100 kN, (c) 200 kN, (d) 300 kN and (e) 400 kN	209
Figure 5.10	Stress distributions in the reinforcement bars of FRP1 column at 5% drift ratio: (a) 70 kN, (b) 100 kN, (c) 200 kN, (d) 300 kN and (e) 400 kN	210

Figure 5.11	Stress distributions in the CFRP stirrups of FRP1 column at 5% drift ratio: (a) 70 kN, (b)100 kN, (c) 200 kN, (d) 300 kN and (e) 400 kN	211
Figure 5.12	The force-stress curves on the concrete surface of SFRP1 column for different axial load intensities	213
Figure 5.13	Stress distributions on the concrete surface for FE models of SFRP1 column at 5% drift ratio: (a) 70 kN, (b)100 kN, (c) 200 kN, (d) 300 kN and (e) 400 kN	214
Figure 5.14	Stress distributions in the reinforcement bars of SFRP1 column at 5% drift ratio: (a) 70 kN, (b)100 kN, (c) 200 kN, (d) 300 kN and (e) 400 kN	215
Figure 5.15	Stress distributions in the CFRP spirals of SFRP1 column at 5% drift ratio: (a) 70 kN, (b)100 kN, (c) 200 kN, (d) 300 kN and (e) 400 kN	216
Figure 5.16	Hysteresis curves of FRP1 column under different intensities of axial load: (a) 70 kN, (b) 100 kN, (c) 200 kN, (d) 300 kN and (e) 400 kN	217
Figure 5.17	Backbone curve of FRP1 column under different intensities of axial	218
Figure 5.18	Hysteresis curves of SFRP1 column under different intensities of axial load: (a) 70 kN, (b) 100 kN, (c) 200 kN, (d) 300 kN and (e) 400 kN	219
Figure 5.19	Backbone curve of SFRP1 column under different intensities of axial load	220
Figure 5.20	The force-stress curves on the concrete surface of FRP1 column for different distance between the stirrups	224
Figure 5.21	Stress distribution on the concrete surface of FRP1 column with different distance between CFRP stirrups at 5% drift ratio: (a) 100 mm, (b)150 mm, (c) 200 mm and (d) 250 mm	225
Figure 5.22	Stress distribution in the reinforcement bars of FRP1 column with different distance between CFRP stirrups at 5% drift ratio: (a) 100 mm, (b)150 mm, (c) 200 mm and (d) 250 mm	226
Figure 5.23	Stress distribution in the CFRP strips of FRP1 column with different distance between stirrups at 5% drift ratio: (a) 100 mm, (b)150 mm, (c) 200 mm and (d) 250 mm	227
Figure 5.24	The force-stress curves on the concrete surface of SFRP1 column for different distance between the spirals	228
Figure 5.25	Stress distribution on the concrete surface of SFRP1 column with different distance between CFRP spirals at 5% drift ratio: (a) 100 mm, (b)150 mm, (c) 200 mm and (d) 250 mm	229



Figure 5.26	Stress distribution in the reinforcement bars of SFRP1 column with different distance between CFRP spirals at 5% drift ratio: (a) 100 mm, (b)150 mm, (c) 200 mm and (d) 250 mm	230
Figure 5.27	Stress distribution in the CFRP strips of SFRP1 column with different distance between spirals at 5% drift ratio: (a) 100 mm, (b)150 mm, (c) 200 mm and (d) 250 mm	231
Figure 5.28	Hysteresis curves of FRP1 column with different distance between CFRP stirrups: (a) 100 mm, (b) 150 mm, (c) 200 mm, (d) 250 mm	232
Figure 5.29	Backbone curves of FRP1 column with different distances between stirrups	232
Figure 5.30	Hysteresis curves of SFRP1 column with different distance between CFRP spirals: (a) 100 mm, (b) 150 mm, (c) 200 mm, (d) 250 mm	234
Figure 5.31	Backbone curves of SFRP1 column with different distances between spirals	234
Figure 6.1	Strain distribution of FRP1 column	241
Figure 6.2	Free body diagram of the applied loads to the FRP1 column	244
Figure 6.3	Strain distribution of SFRP1 column	245
Figure 6.4	Free body diagram of the applied loads to the SFRP1 column	248

## LIST OF ABBREVIATIONS

ACI	-	American Concrete Institute
AFRP	-	Aramid Fibre Reinforced Polymer
ASTM	-	American Society for Testing and Materials
BFRP	-	Basalt Fibre Reinforced Polymer
BS	-	British Standard
CDP	-	Concrete Damage Plasticity
CFL	-	Carbon fibre laminates
CFRP	-	Carbon Fibre Reinforced Polymer
CFST	-	Concrete-filled Stainless-Steel Tubular
CFST	-	Concrete-filled Steel Tubular
CSA	-	Canadian Standards Association
DCH	-	High Ductility Class
DCL	-	Low Ductility Class
DCM	-	Medium Ductility Class
DOT	-	Departments of Transportation
EC	-	Eurocode
FE	-	Finite Element
FEMA	-	Federal Emergency Management Agency
FHWA	-	Federal Highway Administration
GFRP	-	Glass Fibre Reinforced Polymer
HCC	-	Hollow Concrete Column
JBDPA	-	Japan Building Disaster Prevention Association
JSCE	-	Japan Society of Civil Engineers
NaCl	-	Sodium Chloride
OPC	-	Ordinary Portland Cement
RC	-	Reinforced Concrete
SEM	-	Scanning Electron Microscopy
SFCB	-	Steel-FRP Composite Bar
SSTCC	-	Stainless-Steel Tube Confined Concrete

## LIST OF SYMBOLS

$A_{CFRP}$	-	cross-section area of CFRP strips
$A_{con.}$	-	cross-section area of concrete
$A_{rein}$	-	cross-section area of reinforcement
$A_{sw}$	-	cross-section area of transverse reinforcement
$b_w$	-	width of the web on T, I and L beam
$d$	-	effective depth of section
$d_b$	-	nominal diameter of bar, wire, or prestressing strand
$d_{bl,max}$	-	maximum longitudinal bar diameter
$d_{bl,min}$	-	minimum longitudinal bar diameter
$d_w$	-	diameter of stirrups
$E_d$	-	energy dissipated in one cycle
$E_p$	-	the nominal elastic potential energy
$F_y$	-	effective yield strength
$F_u$	-	ultimate lateral force
$h_e$	-	cumulative energy dissipation
$f_{cc}$	-	characteristic compressive strength of concrete
$f_{CFRP}$	-	tensile strength of CFRP
$f_{yh}$	-	yield strength of stirrups
$f'_c$	-	compressive strength of concrete
$l_{cl}$	-	clear length of the column
$l_{cr}$	-	length of critical region
$s$	-	stirrup spacing or pitch of continuous spirals, and longitudinal FRP bar spacing
$w$	-	width of CFRP strip
$\rho$	-	transverse reinforcement ratio
$\epsilon_{cu}$	-	ultimate strain of concrete
$\epsilon_{CFRP}$	-	ultimate strain of CFRP
$\epsilon_{rein.}$	-	strain in the reinforcement
$\epsilon_y$	-	yield strain of reinforcement
$\mu$	-	ductility ratio of displacement $(\frac{\Delta u}{\Delta y})$

- $\Delta_u$  - displacement at ultimate lateral load
- $\Delta_y$  - displacement at effective yield strength
- $^{\circ}\text{C}$  - temperature level

## LIST OF APPENDICES

<b>APPENDIX</b>	<b>TITLE</b>	<b>PAGE</b>
Appendix A	Geometrical Design of CFRP Strips	268
Appendix B	Results of Measured Strain Values	269



# CHAPTER 1

## INTRODUCTION

### 1.1 Introduction

The majority of structures and infrastructures worldwide use reinforced concrete (RC). For many years, carbon steel has been used for making reinforcement bars, hoops and ties. However, in addition to corrosion of steel reinforcements, RC faces other problems which relate to confinement in RC elements. Lateral reinforcements used to confine the longitudinal bars play a vital role in the ultimate load capacity and ductility of RC members like columns (Jing *et al.*, 2016). While corrosion of steel degrades tensile capacity and service life of the structure, improper design and inadequate transverse reinforcement may lead to buckling of main rebars and shear failure (Murray, 2013; Goretti *et al.*, 2017). In many existing columns, lateral reinforcement is provided using 6 to 8 mm diameter bars with 90° hooks at about 200-250 mm spacing (Kaushik and Jain, 2007). As can be seen from Figure 1.1, these RC columns are vulnerable when subjected to severe ground motions.

As Figure 1.2 shows, in recent decades, the usage of Fibre-Reinforced-Polymer (FRP) has significantly increased due to its durability, higher strength-to-weight ratio and ability to be formed in any shape and size (Tamon, 2005; Burgoyne, 2009). The FRP bars have been introduced to replace steel bars as longitudinal reinforcements and stirrups due to their high corrosive resistance (Mohamed *et al.*, 2014; Maranan *et al.*, 2018). So far, researchers have studied the effect of externally bonded FRP sheets on the increase in the axial load capacity of columns.

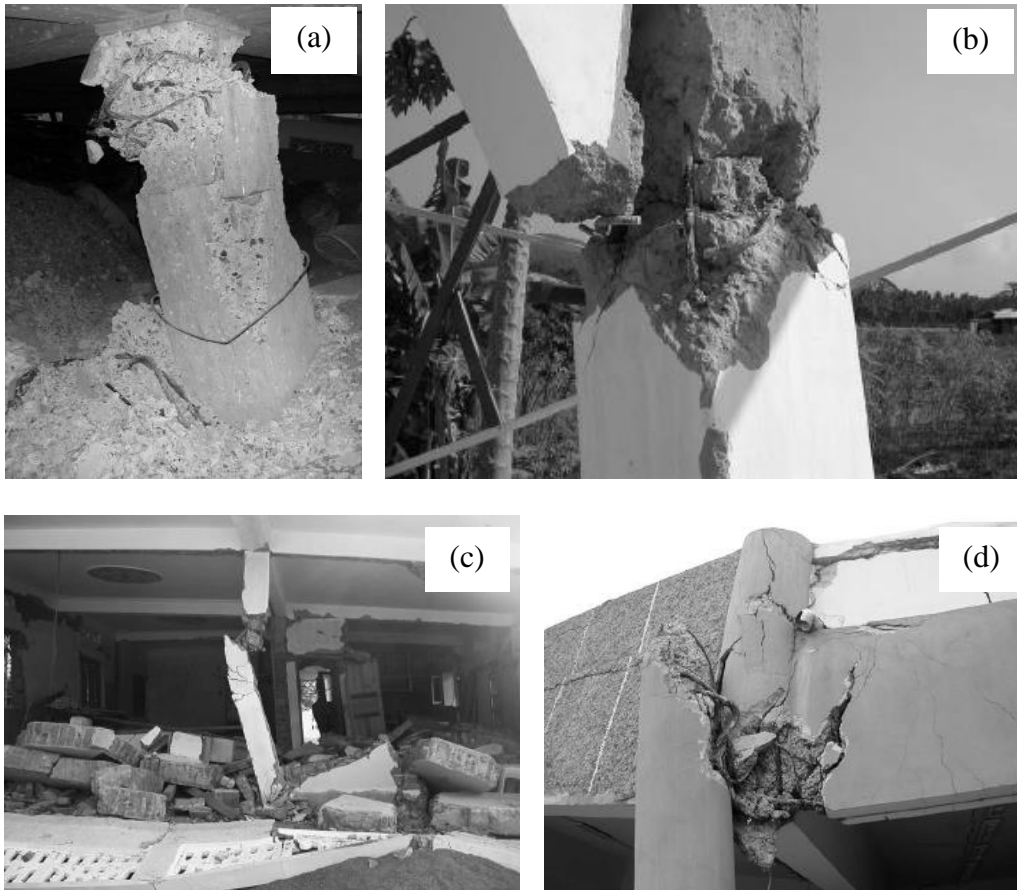


Figure 1.1 Columns failure in RC buildings due to poor shear design during 2004 Sumatra Earthquake and Tsunami; (a), (b) and (c) buckling of longitudinal bars due to 90° hooks opened up and (d) shear failure of column at beam-columns joint (Kaushik and Jain, 2007)



Figure 1.2 FRP sheets wrapped around RC parts to enhance shear and flexure strength; (a) columns and (b) garage beams (Alkhrdaji, 2015)

Due to the potential of FRP composites in RC construction, the application of FRP has become an interesting topic among researchers. Several design guidelines



have been published including ACI 440.1R-15 (2015), ACI 440.2R-08 (2008), CAN/CSAS806-12 (2012), CSA-S806-02 (2002), CNR-DT 202 (2005, 2004) and CNR-DT 204 (2006, 2007). Some studies on durability of FRP composites have also been conducted under harsh environment and severe loadings. So far, FRP composites show good durability in accelerated aging test and excellent response under cyclic load, blast load, and impact load.

This study is conducted to investigate the behaviour of internally confined RC columns by FRP strips under a constant axial load and cyclic lateral loading. The failure mode, ultimate load capacity, ductility and energy dissipation capacity of columns were studied experimentally. Numerical studies were performed to investigate the effect of different intensities of axial load and different configuration of FRP strips on the cyclic response of columns.

## **1.2 Problem Statement**

Axial load capacity of RC columns is directly related to the confinement condition that is provided for concrete (Mander *et al.*, 1988). As can be seen from Figure 1.3, the higher the confinement rate in concrete the higher its compressive strength. Therefore, columns with a better confinement condition have a higher axial load capacity (Mohamed *et al.*, 2014). In general, confined condition for concrete in RC columns is provided through transverse reinforcements (Vellenas *et al.*, 1977; Scott *et al.*, 1982; Mander *et al.*, 1988). Transverse reinforcements that can also increase the shear force capacity can be in the shape of circular hoops, spirals and cross ties. For many years, carbon steel has been used for making the reinforcement bars, hoops and ties. Different shapes, types, cross-section and arrangement of transverse reinforcement contribute to different level of confinement (Mander *et al.*, 1988). However, one main problem with carbon steel stirrups is its corrosion in humid and harsh environmental condition (Apostolopoulos and Papadakis, 2008; Zhao *et al.*, 2018). Figure 1.4 shows an example of corroded stirrups in RC columns. The corroded stirrups have caused the loss of bond between reinforcement and concrete (Tapan *et al.*, 2016). Thus, the axial load carrying capacity of the column decreased due to the

loss of core concrete confinement and heavily cracks of concrete cover. This can be seen in Figure 1.5, where the compressive strength of corroded concrete is lower than the compressive strength of uncorroded concrete.

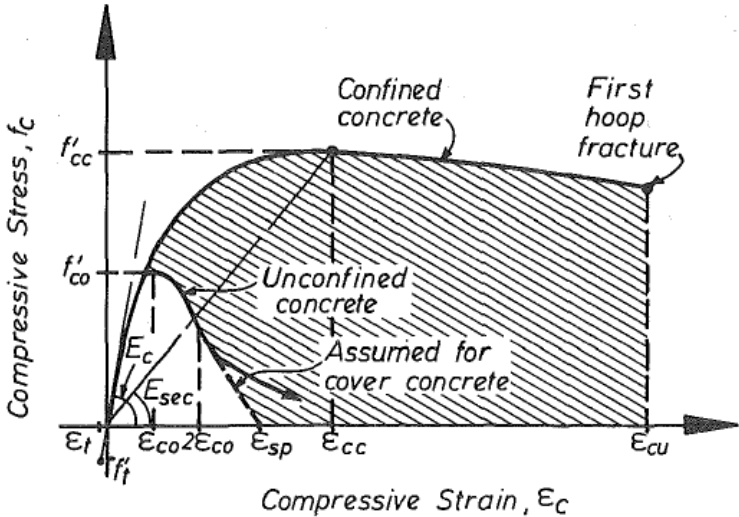


Figure 1.3 Typical stress-strain curves of confined and unconfined concrete (Mander *et al.*, 1988)

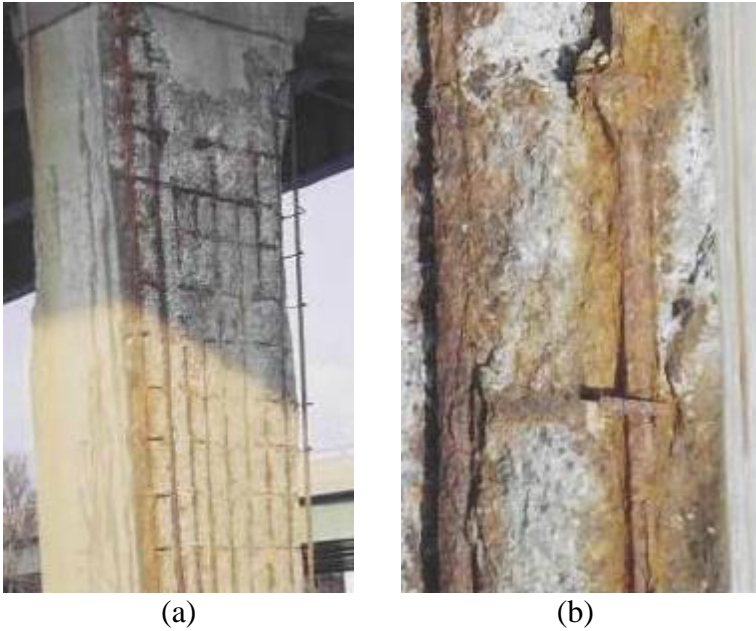


Figure 1.4 Corrosion damage of RC columns; (a) completed deteriorated of stirrups and (b) severe damage of steel rebars (Tapan *et al.*, 2016)

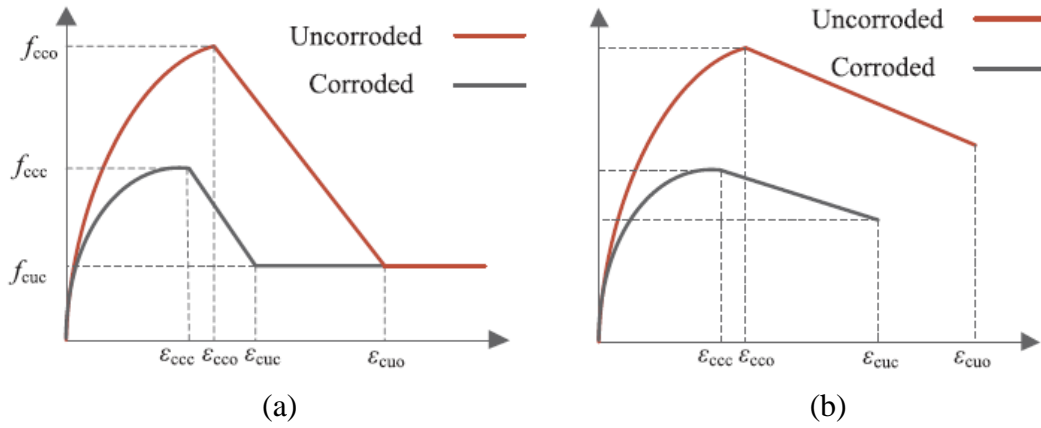


Figure 1.5 The compressive strength of (a) corroded core concrete and (b) corroded concrete cover (Yu *et al.*, 2020)

Another main issue with confinement in RC element is the improper design and inadequate transverse reinforcement which may lead to structural failure during earthquake (Lynn *et al.*, 1996; Alih and Vafaei, 2019). As can be seen from Figure 1.5 and 1.6, large spacing between stirrups and the usage of 90° hooks have been found in many of the damaged columns during past earthquakes. In addition, according to Bikçe and Çelik, (2016), failure analysis of newly constructed RC buildings designed according to 2007 Turkish Seismic Code (TEC) during the October 23, 2011 Van earthquake were severely damaged. Based on the analysis, it was found that the building has not been constructed in accordance with the project and thereby TEC 2007. Inadequate stirrups without crossties, and short length and insufficiently dilatation of hooks have been found in the damaged columns. This shows difficulties to designers and engineers to ensure the implementation of the restrictions stated in the design codes during construction.

Nowadays, when it comes to corrosion problems of carbon steel reinforcements, two options are available: a) usage of stainless-steel reinforcements and b) application of Fibre Reinforced Polymers (FRP) (Burgoyne, 2009; Alih and Khelil, 2012). The main issue with stainless steel reinforcements is related to their expensive cost compared to carbon steel and FRPs. Usage of FRP bar as the replacement for carbon steel reinforcements has been studied by other researchers (Mohamed *et al.*, 2014; Kosmidou *et al.*, 2018; Maranan *et al.*, 2018). Many studies have investigated the effect of externally mounted FRP sheets on the increase in the axial load capacity and the dynamic performance of columns (Kim *et al.*, 2013; Jiang

*et al.*, 2016; Alotaibi and Galal, 2017; Campione *et al.*, 2018). Previous investigations have mostly been conducted for the purpose of retrofitting of existing columns and promising results were obtained. However, so far, there is very limited study has investigated the usage of FRP strips for the internal confinement of RC columns (Tahir *et al.*, 2019). Therefore, this study investigates the cyclic behaviour of concrete columns internally confined by carbon fibre reinforced polymer (CFRP).

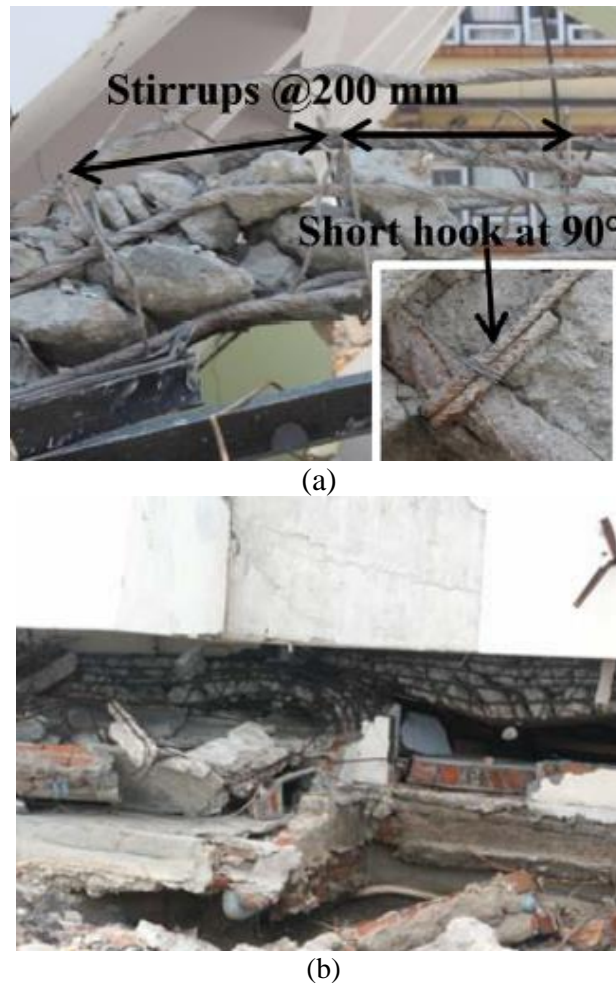


Figure 1.6 Large spacing between the stirrups lead to column failure; (a) damaged column during 2015 Gorkha Earthquake and (b) column failure lead to building collapses during 2004 Sumatra Earthquake and Tsunami (Saatcioglu *et al.*, 2005; Sharma *et al.*, 2016)

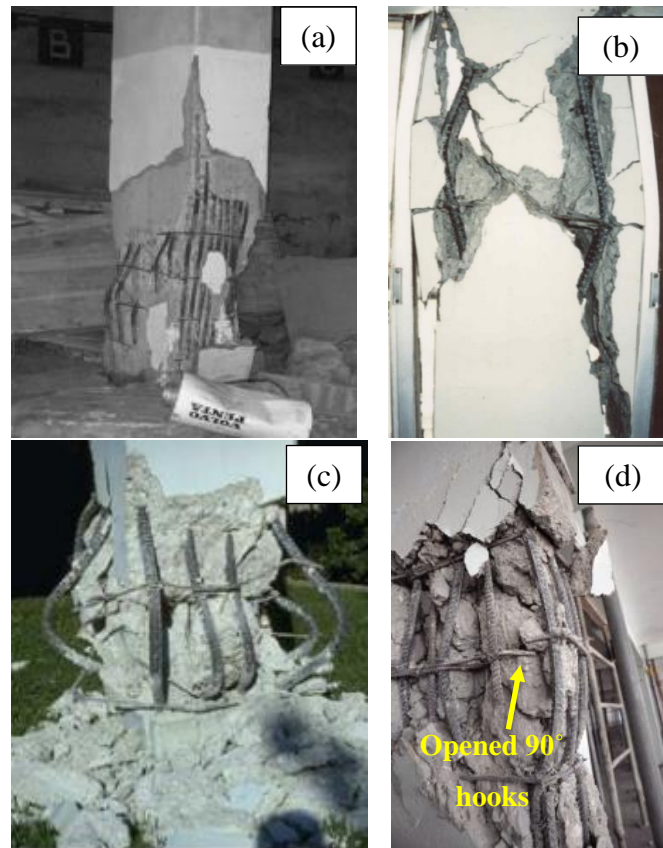


Figure 1.6 Buckling of longitudinal reinforcement during earthquakes due to improper detailing of confinement; (a) Expo building, Talcahuano during 2010 Chile Earthquake and Tsunami, (b) Van Nuys Holiday Inn building, California 1994 Northridge Earthquake, (c) Imperial County Services building California 1994 Northridge Earthquake and (d) Parking garage of the Digicel building 2010 Haiti earthquake (Olsen *et al.*, 2010; Faison *et al.*, 2004; Paultre *et al.*, 2013)

It should be mentioned that CFRP strips have superior properties compared to the mild steel used as stirrups in conventional designs (Quiertant and Clement, 2011; Alsayed *et al.*, 2014; Chellapandian *et al.*, 2017). Table 1.1 shows the comparison between these two materials. As can be seen, CFRP composites have more than 10 times the tensile strength and are 60 times lighter than the carbon mild-steel reinforcements used in conventional stirrups. Not only is the CFRP superior in terms of tensile strength compared to carbon steel, the light-weight property of FRP will reduce the overall weight of the structure in which it will improve seismic resistance in buildings (Lee *et al.*, 2016; Vandanapu and Krishnamurthy, 2018). This research may be used by practicing engineers and designers and therefore will help reduce maintenance and repair cost. These benefits together with the high resistance of CFRP against corrosion and harsh environment were the motivations for conducting this study.

Table 1.1 Summarised properties of FRP sheets and mild steel grade

Properties	CFRP composites	Mild steel
Modulus of elasticity	200-800 GPa	200 GPa
Density	1.75-1.95 g/cm <sup>3</sup>	7.8 g/cm <sup>3</sup>
Strength	2500-6000 MPa	200-380 MPa
Weight	0.0062 kg/m	0.395 kg/m

### 1.3 Objective of Study

As mentioned earlier, the application of CFRP sheets as a transverse reinforcement in RC columns resulted in many benefits for the construction industry. Therefore, the main objective of this study is to investigate the cyclic response (i.e. ultimate load, ultimate displacement, ductility ratio, energy dissipation, effective yield strength, etc.) of RC columns that have been internally confined with CFRP strips when subjected to a reversed cyclic loading. The following are the specific objectives:

- (a) To experimentally investigate the cyclic response of RC columns internally confined with CFRP strips and compare them with that of carbon steel.
- (b) To numerically determine the effects of different axial force and distance of CFRP strips on the cyclic response of RC columns internally confined with CFRP strips.
- (c) To analytically propose a method for estimating the ultimate load of RC columns internally confined with CFRP strips.

### 1.4 Scope of Study

This study focused on the cyclic response of reinforced concrete columns internally confined with CFRP strips. Experimental works were conducted on eight full-scale RC columns with the height of 1500 mm and cross-sectional size of 200 mm x 200 mm. The samples consisted of two main groups: a) three columns with CFRP

stirrups and b) three columns with CFRP spirals. For the sake of comparison, two columns were confined with carbon steel stirrups and spirals with the spacing of 100 mm as reference samples. The compressive strength of concrete used in this study was 25 MPa. The yield strengths of steel bars with the diameter of 12 and 6 mm were 391 and 563 N/mm<sup>2</sup>, respectively. In this study, columns confined with stirrups were reinforced with four longitudinal reinforcement bars, while six longitudinal reinforcement bars were employed in columns confined with spirals. Carbon fibre reinforced polymer (CFRP) sheets with the tensile strength of 4900 MPa were used in this study. In order to study the effect of thickness and distance between the CFRP strips, two samples were constructed and tested using a double layer of CFRP strips with 150 mm distance between the strips, respectively. The column samples were tested experimentally under a constant axial load together with a cyclic load based on FEMA 461 loading protocol. Moreover, in order to conduct a parametric study on the cyclic response of RC columns, a nonlinear analysis by means of Finite Element (FE) software ABAQUS 6.14 was performed. In the numerical study, different intensities of axial loads and different configurations of CFRP strips were investigated. An analytical method was proposed for estimating the ultimate load of columns internally confined by CFRP strips.

## **1.5 Significance of Study**

This study examined the efficiency of CFRP strips to be used as the replacement for conventional carbon steel stirrups in RC columns. The outcome of this research can reduce the corrosion problem as well as increase the axial load capacity of the columns. By using CFRP composites in concrete structures, the dynamic behaviour of RC columns can also be improved. Easy installation and construction of CFRP strips as transverse reinforcement allow designers and engineers to make sure that the real design is implemented during the construction process. This is important because lack of attention to the implementation of the restrictions given in the design codes could cause failure of the building when subjected to severe loading such as earthquake.

## **1.6 Outline of the Thesis**

This thesis consists of seven chapters. The arrangement of the chapter is as follows:

Chapter 1 describes the introduction of the study, the problem statement, the objectives, and the scope of the study, and explains the significance of this research.

Chapter 2 presents the literature review regarding the failure of columns due to seismic events and existing guidelines for the seismic design of columns, as well as the effect of steel corrosion in concrete. A detailed explanation about FRP composites reinforced concrete members and the durability of FRP under harsh environment are presented in this chapter. Advantages and disadvantages of FRP composites are discussed in this chapter as well.

Chapter 3 describes the methodology employed for achieving the defined objectives. The details of experimental works and their properties are explained in this chapter. This chapter also explains about the test setup and the employed loading protocol. It also describes the procedure of numerical studies and analytical calculations.

Chapter 4 discusses the obtained results from the experimental tests. The failure mechanism of columns, ultimate load, ductility and energy dissipation capacity of each sample are calculated and explained in this chapter.

Chapter 5 describes the numerical analysis used to conduct a parametric study on the CFRP strip internally confined RC columns. Validation of Finite element models is presented in this chapter. Results of the parametric study which included the effect of different intensities of axial load and different configurations of FRP strips are presented in this chapter.



Chapter 6 presents the proposed method for analytical calculation of ultimate load of RC columns internally confined with CFRP strips. The comparison between analytical and experimental results is also presented in this chapter.

Finally, Chapter 7 summarises and concludes the entire thesis. The research findings, contributions of the thesis and recommendations for future work are also discussed in this chapter.

## REFERENCES

- ABAQUS (2014) 'Simulia DS. Abaqus 6.14 Documentation'. Providence, RI, USA.
- Abdel-Mooty, M. A. N., Issa, M. E., Farag, H. M. and Bitar, M. A. (2006) 'Seismic upgrading of square and rectangular RC columns using FRP wrapping', *High Performance Structures and Materials III*, 85, pp. 419–428.
- ACI 318-02 (2002) *Building code requirements for structural concrete*. Farmington Hills, Detroit, Michigan, USA, American Concrete Institute.
- ACI 440.1R-15 (2015) *Guide for the Design and Construction of Structural Concrete Reinforced with Fibre-Reinforced Polymer (FRP) Bars*. Farmington Hills, Detroit, Michigan, USA, American Concrete Institute.
- ACI 440.2R-08 (2008) *Guidelines for the Design and Construction of Externally Bonded FRP Systems for Strengthening Existing Structures*, American Concrete Institute ACI Committee 440. Italy: Italian National Research Council.
- Al-nimry, H. and Neqresh, M. (2019) 'Confinement effects of unidirectional CFRP sheets on axial and bending capacities of square RC columns', *Engineering Structures journal*, 196, p. 109329.
- Ali, A. H., Mohamed, H. M., Chaallal, O., Benmokrane, B. and Ghrib, F. (2018) 'Shear resistance of RC circular members with FRP discrete hoops versus spirals', *Engineering Structures*, 174, pp. 688–700.
- Alih, S. C. and Vafaei, M. (2019) 'Performance of reinforced concrete buildings and wooden structures during the 2015 Mw 6.0 Sabah earthquake in Malaysia', *Engineering Failure Analysis journal*, 102, pp. 351–368.
- Alih, S. and Khelil, A. (2012) 'Behavior of inoxydable steel and their performance as reinforcement bars in concrete beam: Experimental and nonlinear finite element analysis', *Construction and Building Materials*, 37, pp. 481–492.
- Alkhrdaji, T. (2015) 'Strengthening of Concrete Structures Using FRP Composites', *Building Blocks*, pp. 18–20.
- Alotaibi, K. S. and Galal, K. (2017) 'Axial compressive behavior of grouted concrete block masonry columns confined by CFRP jackets', *Composites Part B: Engineering*, 114, pp. 467–479.

- Alsayed, S. H., Almusallam, T. H., Ibrahim, S. M., Al-Hazmi, N. M., Al-Salloum, Y. A. and Abbas, H. (2014) 'Experimental and numerical investigation for compression response of CFRP strengthened shape modified wall-like RC column', *Construction and Building Materials*, 63, pp. 72–80.
- Apostolopoulos, C. A. and Papadakis, V. G. (2008) 'Consequences of steel corrosion on the ductility properties of reinforcement bar', *Construction and Building Materials*. Elsevier, 22(12), pp. 2316–2324.
- Ashrafi, H., Bazli, M., Pournamazian, E. and Vatani, A. (2017) 'The effect of mechanical and thermal properties of FRP bars on their tensile performance under elevated temperatures', *Construction and Building Materials*. Elsevier Ltd, 157, pp. 1001–1010.
- ASTM D3039/D 3039M–08 (2008) *Standard test method for tensile properties of polymer-matrix composite materials*.
- ASTM D3916-94 (2002) *Standard Test Method for Tensile Properties of Pultruded Glass-Fiber-Reinforced Plastic Rod*. ASTM International, West Conshohocken, PA.
- Attari, N., Si, Y. and Amziane, S. (2019) 'Seismic performance of reinforced concrete beam – column joint strengthening by frp sheets', *Structures*, 20(December 2018), pp. 353–364.
- Augenti, N., Nanni, A. and Parisi, F. (2013) 'Construction Failures and Innovative Retrofitting', *Buildings*, pp. 100–121.
- Baker, M. (2018) 'How to get meaningful and correct results from your finite element model', pp. 1–26.
- Bank, L. C., Puterman, M. and Katz, A. (1998) 'Effect of material degradation on bond properties of fiber reinforced plastic reinforcing bars in concrete', *ACI Mater J*, 95(3), pp. 232–43.
- Behnam, H., Kuang, J. S. and Samali, B. (2018) 'Parametric finite element analysis of RC wide beam-column connections', *Computers and Structures*, 205, pp. 28–44.
- Bikçe, M. and Çelik, T. B. (2016) 'Failure analysis of newly constructed RC buildings designed according to 2007 Turkish Seismic Code during the October 23 , 2011 Van earthquake', *EFA*. Elsevier Inc., 64, pp. 67–84.
- Bokey, P. B. and Pajgade, P. S. (2004) 'Lessons From Jan, 26, 2001 Gujrat (India) Earthquake', *Structure*, 444606(1874).

- BS 8110 (1985) *Structural use of concrete—code of practice for design and construction*. British standards institution.
- Buildings Department (2004) *Code of practice for structural use of concrete. Second Ed. Hong Kong: The Government of the Hong Kong Special Administrative Region*.
- Burgoyne, C. (2009) ‘Fibre Reinforced Polymers – Strengths, Weaknesses, Opportunities and Threats’, in *FRPRCS-9*. Sydney, Australia, pp. 1–6.
- Campione, G., Cannella, F., Ferrotto, M. F. and Gianquinto, M. (2018) ‘Compressive behavior of FRP externally wrapped RC column with buckling effects of longitudinal bars’, *Engineering Structures*, 168(April), pp. 809–818.
- CAN/CSA-S6-14 (2014) *Canadian highway bridge design code*. Rexdale, Ontario, Canada: Canadian Standards Association (CSA).
- CAN/CSAS806-12 (2012) *Design and construction of building components with fiber reinforced polymers*. Rexdale, Ontario, Canada.
- Chellapandian, M., Suriya Prakash, S. and Sharma, A. (2017) ‘Strength and Ductility of Innovative Hybrid NSM Reinforced and FRP Confined Short RC Columns under Axial Compression’, *Composite Structures*, 176, pp. 205–216.
- Chen, Y., Davalos, J. F., Ray, I. and Kim, H. (2007) ‘Accelerated aging tests for evaluations of durability performance of FRP reinforcing bars for concrete structures’, *Composite Structures*, 78, pp. 101–111.
- Cheng, J., Luo, X. and Xiang, P. (2020) ‘Experimental study on seismic behavior of RC beams with corroded stirrups at joints under cyclic loading’, *Journal of Building Engineering*. Elsevier Ltd, 32(September 2019), p. 101489.
- Chopra, A. K. (1995) *Dynamics of structures: Theory and applications to earthquake engineering*. Englewood Cliffs, N.J: Prentice Hall.
- CNR-DT 202/2005 (2004) *Guide for the design and construction of externally bonded FRP systems for strengthening existing structures*. Italy.
- CNR-DT 204/2006 (2007) *Guide for the Design and Construction of Fiber-Reinforced Concrete Structures*. Italy.
- Colomb, F., Tobbi, H., Ferrier, E. and Hamelin, P. (2008) ‘Seismic retrofit of reinforced concrete short columns by CFRP materials’, *Composite Structures*, 82(4), pp. 475–487.
- CSA-S806-02 (2002) *Design and Construction of Building Components with Fibre-Reinforced Polymers, CSA-S806-02*.

- Damchevski, B. (2016) *Repair of reinforced concrete structures in compliance with the European Standard EN 1504*.
- Del, M., Di, M., Balsamo, A. and Prota, A. (2017) 'FRP for seismic strengthening of shear controlled RC columns : Experience from earthquakes and experimental analysis', *Composites Part B*, 129.
- Delgado, P., Arêde, A., Vila Pouca, N., Rocha, P., Costa, A. and Delgado, R. (2012) 'Retrofit of RC hollow piers with CFRP sheets', *Composite Structures*, 94(4), pp. 1280–1287.
- El-Sayed, A. K., Hussain, R. R. and Shuraim, A. B. (2015) 'Effect of Stirrup Corrosion on the Shear Strength of Reinforced Concrete Short Beams', *Journal of Civil Engineering and Management*, 22(4), pp. 491–499.
- Faison, H., Comartin, C. and Elwood, K. (2004) 'Reinforced concrete moment frame building without seismic details', *World Housing Encyclopedia*.
- FEMA 356 (2000) *Prestandard and Commentary for the Seismic Rehabilitation of Buildings*. Washington DC.
- FEMA 461 (2007) *Interim Testing Protocols for Structural and Nonstructural Performance Characteristics of Determining the Seismic Components*. Redwood City, California.
- Fukuyama, H., Tumialan, G. and Nanni, A. (2001) 'Japanese Design And Construction Guidelines for Seismic Retrofit of Buildings Structures with FRP Composites', pp. 107–118.
- Giamundo, V., Lignola, G. P., Prota, A. and Manfredi, G. (2014) 'Analytical Evaluation of FRP Wrapping Effectiveness in Restraining Analytical Evaluation of FRP Wrapping Effectiveness in Restraining Reinforcement Bar Buckling', *Journal of Structural Engineering*, p. 12.
- Goretti, A., Molina Hutt, C. and Hedelund, L. (2017) 'Post-earthquake safety evaluation of buildings in Portoviejo, Manabí province, following the Mw7.8 Ecuador earthquake of April 16, 2016', *International Journal of Disaster Risk Reduction*, 24, pp. 271–283.
- Grammatikos, S. A., Evernden, M., Mitchels, J., Zafari, B., Mottram, J. T. and Papanicolaou, G. C. (2016) 'On the response to hygrothermal aging of pultruded FRPs used in the civil engineering sector', *Materials and Design*, 96, pp. 283–295.

- Günaslan, S. E., Karaşin, A. and Öncü, M. E. (2014) ‘Properties of FRP Materials for Strengthening’, *International Journal of Innovative Science, Engineering & Technology*, 1(9), pp. 656–660.
- Guo, Y., Gao, W., Zeng, J., Duan, Z., Ni, X. and Peng, K. (2019) ‘Compressive behavior of FRP ring-confined concrete in circular columns: Effects of specimen size and a new design-oriented stress-strain model’, *Construction and Building Materials*, 201, pp. 350–368.
- Hamad, R. J. A., Megat Johari, M. A. and Haddad, R. H. (2017) ‘Mechanical properties and bond characteristics of different fiber reinforced polymer rebars at elevated temperatures’, *Construction and Building Materials*, 142, pp. 521–535.
- Hawileh, R. A., Abu-obeidah, A., Abdalla, J. A. and Al-tamimi, A. (2015) ‘Temperature effect on the mechanical properties of carbon , glass and carbon – glass FRP laminates’, *Construction and Building Materials*, 75, pp. 342–348.
- He, M., Tao, D., Li, Z. and Li, M. (2016) ‘Mechanical Behavior of Dowel-Type Joints Made’, *Materials*, 9(581).
- Hoffard, T. a and Malvar, L. J. (2005) *Fiber-Reinforced Polymer Composites in Bridges: A State-of-the-Art Report*. California.
- Inel, M. and Ozmen, H. B. (2006) ‘Effects of plastic hinge properties in nonlinear analysis of reinforced concrete buildings’, *Engineering Structures*, 28, pp. 1494–1502.
- JBDPA (2005) *Recent Development of Seismic Retrofit Methods in Japan, English*. Japan Building Disaster Prevention Association.
- Jiang, S. F., Zeng, X., Shen, S. and Xu, X. (2016) ‘Experimental studies on the seismic behavior of earthquake-damaged circular bridge columns repaired by using combination of near-surface-mounted BFRP bars with external BFRP sheets jacketing’, *Engineering Structures*, 106, pp. 317–331.
- Jing, D. H. H., Yu, T. and Liu, X. D. D. (2016) ‘New configuration of transverse reinforcement for improved seismic resistance of rectangular RC columns: Concept and axial compressive behavior’, *Engineering Structures*. Elsevier, 111, pp. 383–393.
- Johar, M., Kosnan, M. S. E. and Tamin, M. N. (2014) ‘Cyclic Cohesive Zone Model for Simulation of Fatigue Failure Process in Adhesive Joints’, in *Materials, Industrial and Manufacturing Engineering Research Advances*, pp. 217–221.

- JSCE (1997) *Recommendation for design and construction of concrete structures using continuous fiber reinforcing materials*. Tokyo: Japan Society of Civil Engineers (JSCE).
- Kaplan, H., Yilmaz, S., Binici, H., Yazar, E. and Cetinkaya, N. (2004) ‘May 1 2003 Turkey Bingol earthquake damage in reinforced concrete structures.pdf’, *Engineering Failure Analysis*, 11, pp. 279–291.
- Kaushik, H. B. and Jain, S. K. (2007) ‘Impact of Great December 26, 2004 Sumatra Earthquake and Tsunami on Structures in Port Blair’, *Journal of Performance of Constructed Facilities*, 21(2), pp. 128–142.
- Kim, J., Kwon, M., Jung, W. and Limkatanyu, S. (2013) ‘Seismic performance evaluation of RC columns reinforced by GFRP composite sheets with clip connectors’, *Construction and Building Materials*, 43, pp. 563–574.
- Kobayashi, A., Hidekuma, Y. and Saito, M. (2009) ‘Application of the Frp for Construction As High Durability Materials in Japan’, *Proceedings of US-Japan Workshop on Life Cycle Assessment of Sustainable Infrastructure Materials*, pp. 1–9.
- Kosmidou, P. K., Chalioris, C. E. and Karayannis, C. G. (2018) ‘Flexural / shear strength of RC beams with longitudinal FRP bars An analytical approach’, *Computers and Concrete*, 6, pp. 573–592.
- Kumar, R., Iwanami, M., Chijiwa, N. and Uno, K. (2020) ‘Effect of non-uniform rebar corrosion on structural performance of RC structures: A numerical and experimental investigation’, *Construction and Building Materials*. Elsevier Ltd, 230, p. 116908.
- Lee, J. and Fenves, G. L. (1998) ‘Plastic-damage model for cyclic loading of concrete structures’, *J Eng Mech.*, 124, pp. 892–900.
- Lee, K. S., Lee, B. Y. and Seo, S. Y. (2016) ‘A Seismic Strengthening Technique for Reinforced Concrete Columns Using Sprayed FRP’, *Polymers*, 8(107), p. 21.
- Li, Q., Niu, D. tao, Xiao, Q. hui, Guan, X. and Chen, S. jie (2018) ‘Experimental study on seismic behaviors of concrete columns confined by corroded stirrups and lateral strength prediction’, *Construction and Building Materials*. Elsevier, 162, pp. 704–713.
- Lublinter, J., Oliver, J., Oller, S. and Oñate, E. (1989) ‘A plastic-damage model for concrete’, *Int J Solids Struct.*, 25, pp. 299–326.

- Luna, M. F. J., Alonso, A. M. C., Sánchez, M. M. and Jarabo, C. R. (2017) ‘Corrosion protection of galvanized rebars in ternary binder concrete exposed to chloride penetration’, *Construction and Building Materials*, 156, pp. 468–475.
- Luo, X., Cheng, J., Xiang, P. and Long, H. (2020) ‘Seismic behavior of corroded reinforced concrete column joints under low - cyclic repeated loading’, *Archives of Civil and Mechanical Engineering*. Springer London, 20(2), pp. 1–20.
- Lynn, A. C., Moehle, J. P., Mahin, S. A. and Holmes, W. T. (1996) ‘Seismic Evaluation of Existing Reinforced Concrete Building Columns’, *Earthquake Spectra*, 12(4), pp. 715–739.
- Ma, G., Li, H., Yan, L. and Huang, L. (2018) ‘Testing and analysis of basalt FRP-confined damaged concrete cylinders under axial compression loading’, *Construction and Building Materials*, 169, pp. 762–774.
- Maljaee, H., Ghiassi, B., Lourenço, P. B. and Oliveira, D. V (2016) ‘FRP – brick masonry bond degradation under hygrothermal conditions’, *Composite Structures*, 147, pp. 143–154.
- Mander, J. B., Priestley, M. J. N. and Park, R. (1988) ‘Theoretical Stress-Strain Model for Confined Concrete’, *Journal of Structural Engineering*, pp. 1804–1826.
- Mansouri, L., Djebbar, A., Khatir, S. and Abdel, M. (2019) ‘Effect of hygrothermal aging in distilled and saline water on the mechanical behaviour of mixed short fibre/woven composites’, *Composite Structures*, 207, pp. 816–825.
- MAPEI Malaysia (2018) *MapeWrapC UNI-A*. MAPEI Malaysia Sdn. Bhd.
- Maranan, G. B., Manalo, A. C., Benmokrane, B., Karunasena, W., Mendis, P. and Nguyen, T. Q. (2018) ‘Shear behaviour of geopolymer-concrete beams transversely reinforced with continuous rectangular GFRP composite spirals’, *Composite Structures*, 187, pp. 454–465.
- McGurn, J. F. (1998) ‘Stainless Steel Reinforcing Bars in Concrete’, in *The International Conference on Corrosion and Rehabilitation of Reinforced Concrete Structures*. Orlando.
- Micelli, F. and Nanni, A. (2004) ‘Durability of FRP rods for concrete structures’, *Construction and Building Materials*, 18(7), pp. 491–503.
- Mohamed, H. M., Mohammad, Z. A. and Benmokrane, B. (2014) ‘Performance Evaluation of Concrete Columns Reinforced Longitudinally with FRP Bars



- and Confined with FRP Hoops and Spirals under Axial Load', *J. Bridge Eng.*, (2003), pp. 1–12.
- Mojarradbahreh, V. and El-badry, M. (2014) 'Reinforcing Beam-Column Joints with Steel Headed Studs for Seismic Resistance', in *International Van Earthquake Symposium*. Van, Turkey, pp. 1–9.
- Mulas, M. G., Perotti, F., Coronelli, D., Martinelli, L. and Paolucci, R. (2013) 'The partial collapse of "Casa dello Studente" during L'Aquila 2009 earthquake', *Engineering Failure Analysis*. Pergamon, 34, pp. 566–584.
- Murray, J. . A. and Sasani, M. (2013) 'Seismic shear-axial failure of reinforced concrete columns vs. system level structural collapse', *Engineering Failure Analysis*, 32.
- Najafabadi, E. P., Oskouei, A. V., Khaneghahi, M. H., Shoaee, P. and Ozbakkaloglu, T. (2019) 'The tensile performance of FRP bars embedded in concrete under elevated temperatures', *Construction and Building Materials*. Elsevier Ltd, 211, pp. 1138–1152.
- Nakada, M. and Miyano, Y. (2009) 'Accelerated testing for long-term fatigue strength of various FRP laminates for marine use', 69, pp. 805–813.
- Namita (2018) *Effects of corrosion in reinforcement, Civil Digital*.
- Olsen, M. J., Cheung, K. F., Yamazaki, Y., Butcher, S., Garlock, M., Yim, S. C., Piaskowy, S., Robertson, I., Young, Y. L. and Hall, O. (2010) *Damage Assessment of the 2010 Chile Earthquake and Tsunami using Ground-based LIDAR*.
- Ouyang, L. J., Gao, W. Y., Zhen, B. and Lu, Z. D. (2017) 'Seismic retrofit of square reinforced concrete columns using basalt and carbon fiber-reinforced polymer sheets: A comparative study', *Composite Structures*, 162, pp. 294–307.
- Pam, H. J. and Ho, J. C. M. (2009) 'Length of critical region for confinement steel in limited ductility high-strength reinforced concrete columns', *Engineering Structures*, 31(12), pp. 2896–2908.
- Paultre, P., Calais, E. and Proulx, J. (2013) 'Damage to engineered structures during the January 12, 2010, Haiti (Léogane) earthquake', *Can. J. Civ. Eng.*, 40, pp. 1–14.
- Pradhan, B. (2014) 'Corrosion behavior of steel reinforcement in concrete exposed to composite chloride – sulfate environment', *Construction and Building Materials*, 72, pp. 398–410.

- Priestley, M., Seible, F. and Calvi, G. (1996) *Seismic design and retrofit of bridges*. New York: John Wiley & Sons.
- Quagliarini, E., Monni, F., Bondioli, F. and Lenci, S. (2016) 'Basalt fiber ropes and rods: Durability tests for their use in building engineering', *Journal of Building Engineering*, 5, pp. 142–150.
- Quiertant, M. and Clement, J. L. (2011) 'Behavior of RC columns strengthened with different CFRP systems under eccentric loading', *Construction and Building Materials*, 25(2), pp. 452–460.
- Rabi, M., Cashell, K. A. and Shamass, R. (2019) 'Flexural analysis and design of stainless steel reinforced concrete beams', *Engineering Structures*. Elsevier, 198, p. 109432.
- Rajput, A. S. and Sharma, U. K. (2018) 'Corroded reinforced concrete columns under simulated seismic loading', *Engineering Structures*, 171, pp. 453–63.
- Rousakis, T. C. and Karabinis, A. I. (2012) 'Adequately FRP confined reinforced concrete columns under axial compressive monotonic or cyclic loading', *Materials and Structures*, 45(7), pp. 957–975.
- Ruiz-Pinilla, J. G., Adam, J. M., Perez-Carcel, R., Yuste, J. and Moragues, J. J. (2016) 'Learning from RC building structures damaged by the earthquake in Lorca, Spain, in 2011', *Engineering Failure Analysis*, 68, pp. 76–.
- Saatcioglu, M., Ghobarah, A. and Nistor, I. (2005) 'Effects of the December 26 , 2004 Sumatra Earthquake and Tsunami on Physical Infrastructure', *Journal of Earthquake Technology*, 42(4), pp. 79–94.
- Sadone, R., Quiertant, M., Mercier, J. and Ferrier, E. (2012) 'Experimental study on RC columns retrofitted by FRP and subjected to seismic loading', in *6th Int conf on FRP compos in civil eng (CICE)*. Rome, pp. 1–9.
- Sathwik, M. C., Prashanth, M. H., Naik, S. C. and Satish, A. (2020) 'Materials Today : Proceedings Experimental and numerical studies on compressive behaviour of CFRP wrapped cylindrical concrete specimens subjected to different pre-loading conditions', *Materials Today: Proceedings*. Elsevier Ltd., 27, pp. 327–335.
- Scott, B. D., Park, R. and Priestley, M. J. N. (1982) 'Stress-strain behavior of concrete confined by overlapping hoops at low and high strain rate', in *Am. Concr. Inst. J.*, pp. 13–27.

- Seible, B. F., Priestley, M. J. N. and Hegemier, G. A. (1997) 'Seismic Retrofit of RC columns with continuous carbon fibre jackets', *Journal of Composites for Construction*, 1(2), pp. 52–62.
- Sen, R. and Mullins, G. (2007) 'Application of FRP composites for underwater piles repair', *Composites: Part B*, 38(5–6), pp. 751–758.
- Shaikh, F. U. A. and Alishahi, R. (2019) 'Behaviour of CFRP wrapped RC square columns under eccentric compressive loading', *Structures journal*, 20, pp. 309–323.
- Sharma, K., Deng, L. and Noguez, C. C. (2016) 'Field investigation on the performance of building structures during the April 25, 2015, Gorkha earthquake in Nepal', *Engineering Structures*, 121, pp. 61–74.
- Shen, Q., Wang, Jingfeng, Wang, Jiaxin and Ding, Z. (2019) 'Axial compressive performance of circular CFST columns partially wrapped by carbon FRP', *Journal of Constructional Steel Research*, 155, pp. 90–106.
- Shi, Jinjie, Ming, J., Sun, W. and Zhang, Y. (2017) 'Corrosion performance of reinforcing steel in concrete under simultaneous flexural load and chlorides attack', *Construction and Building Materials*. Elsevier, 149, pp. 315–326.
- Shi, J., Wang, X., Wu, Z. and Zhu, Z. (2017) 'Fatigue behavior of basalt fiber-reinforced polymer tendons under a marine environment', 137, pp. 46–54.
- Silva, M. A. G., Sena, B. and Biscaia, H. (2014) 'On estimates of durability of FRP based on accelerated tests', *Composite Structures*, 116, pp. 377–387.
- Sugiman, S., Crocombe, A. D. and Aschroft, I. A. (2013) 'Modelling the static response of unaged adhesively bonded structures', *Engineering Fracture Mechanics*, 98, pp. 296–314.
- Sun, Z., Wu, G., Zhang, J., Zeng, Y. and Xiao, W. (2017) 'Experimental study on concrete columns reinforced by hybrid steel-fiber reinforced polymer ( FRP ) bars under horizontal cyclic loading', *Construction and Building Materials*, 130, pp. 202–211.
- Tahir, M., Wang, Z., Majid, K. and Isleem, H. F. (2019) 'Shear behavior of concrete beams reinforced with CFRP sheet strip stirrups using wet-layup technique', *Structures*. Elsevier, 22(July), pp. 43–52.
- Tamon, U. (2005) 'FRP for Construction In Japan', *Joint Seminar on Concrete Engineering*, pp. 54–68.

- Tang, H., Chen, J., Fan, L., Sun, X. and Peng, C. (2020) 'Experimental investigation of FRP-confined concrete-filled stainless steel tube stub columns under axial compression', *Thin-Walled Structures*, 146, p. 106483.
- Tapan, M., Ozvan, A. and Akkaya, I. (2016) 'Effect of Stirrup Corrosion on Concrete Confinement Strength', *International Journal of Civil and Environmental Engineering*, 3(12), pp. 1595–1598.
- Tastani, S., Pantazopoulou, S. J., Asce, M., Zdoumba, D., Plakantaras, V. and Akritidis, E. (2006) 'Limitations of FRP Jacketing in Confining Old-Type Reinforced Concrete Members in Axial Compression', *Journal of Composites for Construction*, 17(February).
- Vahed, Y. K. (2017) *Seismic Retrofit of Low-Ductile Columns Through Concrete Jacketing with Inoxydable Reinforcement*. Universiti Teknologi Malaysia.
- Vandanapu, S. N. and Krishnamurthy, M. (2018) 'Seismic Performance of Lightweight Concrete Structures', *Advances Civil Engineering*, 2018, p. 6.
- Vellenas, J., Bertero, V. V. and Popov, E. P. (1977) *Concrete confined by rectangular hoops subjected to axial loads*. Berkeley, Calif.
- Wang, G., Dai, J. and Bai, Y. (2019) 'Seismic retrofit of exterior RC beam-column joints with bonded CFRP reinforcement : An experimental study', *Composite Structures*, 224(May), p. 111018.
- Wang, X., Petru, M. and Yu, H. (2019) 'The effect of surface treatment on the creep behavior of flax fiber reinforced composites under hygrothermal aging conditions', *Construction and Building Materials*, 208, pp. 220–227.
- Wang, Y. C., Wong, M. H. and Kodur, V. (2003) 'Mechanical properties of fibre reinforced polymer reinforcing bars at elevated temperatures', *Designing Structures for Fire*, pp. 183–192.
- Wang, Z., Wang, D., Smith, S. T. and Lu, D. (2012) 'Experimental testing and analytical modeling of CFRP-confined large circular RC columns subjected to cyclic axial compression', *Engineering Structures*, 40, pp. 64–74.
- Wu, J., Diao, B., Xu, J., Zhang, R. and Zhang, W. (2020) 'Effects of the reinforcement ratio and chloride corrosion on the fatigue behavior of RC beams', *International Journal of Fatigue*. Elsevier, 131, p. 105299.
- Yao, M., Zhu, D., Yao, Y., Zhang, H. and Mobasher, B. (2016) 'Experimental study on basalt FRP / steel single-lap joints under different loading rates and temperatures', *Composite Structures*, 145, pp. 68–79.

- Yu, R., Chen, L., Zhang, D. and Wang, Z. (2020) ‘Life cycle embodied energy analysis of RC structures considering chloride- induced corrosion in seismic regions’, *Structures*. Elsevier, 25(July 2019), pp. 839–848.
- Yuan, F., Wu, Y. and Li, C. (2017) ‘Modelling plastic hinge of FRP-confined RC columns’, *Engineering Structures*, 131, pp. 651–668.
- Zeng, J., Gao, W., Duan, Z., Bai, Y., Guo, Y. and Ouyang, L. (2020) ‘Axial compressive behavior of polyethylene terephthalate / carbon FRP- confined seawater sea-sand concrete in circular columns’, *Construction and Building Materials*, 234, p. 117383.
- Zhang, C. X. (2012) *Experimental and numerical study on seismic performance of new hybrid reinforced concrete-filled fiber reinforced polymer tubes bridge piers*. Fuzhou University.
- Zhang, Y., Tabandeh, A., Ma, Y. and Gardoni, P. (2020) ‘Seismic performance of precast segmental bridge columns repaired with CFRP wraps’, *Composite Structures*, 243(December 2019).
- Zhao, P., Xu, G., Wang, Q., Zhao, J. and Liu, X. (2018) ‘Influence of stirrup arrangements on the corrosion characteristics of reinforced concrete members’, *Construction and Building Materials*, 192, pp. 683–695.
- Zheng, X. H., Huang, P. Y., Chen, G. M. and Tan, X. M. (2015) ‘Fatigue behavior of FRP – concrete bond under hygrothermal environment’, *Construction and Building Materials*, 95, pp. 898–909.
- Zhou, A., Qin, R., Lun, C. and Lau, D. (2019) ‘Structural performance of FRP confined seawater concrete columns under chloride environment’, *Composite Structures*. Elsevier, 216, pp. 12–19.
- Zhou, Y., Liu, X., Xing, F., Cui, H. and Sui, L. (2016) ‘Axial compressive behavior of FRP-confined lightweight aggregate concrete: An experimental study and stress-strain relation model’, *Construction and Building Materials*. Elsevier Ltd, 119, pp. 1–15.

## LIST OF PUBLICATIONS

- Alih, S. C., Khelil, A., Vafaei, M., Hajarul, N. and Abd, F. (2017) ‘Analytical Tension Stiffening Model for Concrete Beam Reinforced with Inoxydable Steel’, *International Journal of Applied Engineering Research*, 12(15), pp. 5280–5288.
- Alih, S. C., Vafaei, M., Mansour, F. R., Hajarul, N. and Abdul, F. (2017) ‘A Numerical Study on the Seismic Performance of Built-Up Battened Columns’, *International Journal of Civil, Environmental, Structural, Construction and Architectural Engineering*, 11(5), pp. 671–674.
- Halim, N. H. F. A., Alih, S. C. and Vafaei, M. (2020) ‘Efficiency of CFRP strips as a substitute for carbon steel stirrups in RC columns’, *Materials and Structures*. Springer Netherlands, 53(129), p. 12.
- Halim, N. H. F. A., Alih, S. C. and Vafaei, M. (2018) ‘Structural behavior of RC columns transversely reinforced with FRP strips’, *International Journal of Civil Engineering and Technology*, 9(4), pp. 1572–1583.
- Halim, N. H. F. A., Alih, S. C., Vafaei, M., Baniahmadi, M. and Fallah, A. (2017) ‘Durability of Fibre Reinforced Polymer under Aggressive Environment and Severe Loading: A Review, International’, *Journal of Applied Engineering Research*, 12(22), pp. 12519–12533.
- Halim, N. H. F. A., Alih, S. C. and Vafaei, M. (2019) ‘Comparison between cyclic response of RC columns transversely reinforced with FRP strips and carbon steel Comparison between cyclic response of RC columns transversely reinforced with FRP strips and carbon steel’, *IOP Conf. Series: Materials Science and Engineering*, 513, p. 8.
- Halim, N. H. F. A., Alih, S. C. and Vafaei, M. (2019) ‘Analytical calculation on shear capacity of RC columns internally confined with CFRP strips Analytical calculation on shear capacity of RC columns internally confined with CFRP strips’, in *IOP Conference Series: Earth and Environmental Science*, pp. 1–9.
- Halim, N. H. F. A., Sophia C. Alih and Vafaei, M. (2018) ‘Shear Capacity of Internally Confined RC Columns with FRP Strips’, in *7th International Graduate Conference of Engineering, Science and Humanities*, pp. 142–144.

Vafaei, M., Alih, S. C., Shad, H., Falah, A., Halim, N. H. F. A. and Abdul, F. (2018)  
‘Prediction of strain values in reinforcements and concrete of a RC frame using  
neural networks’, *International Journal of Advanced Structural Engineering*.  
Springer Berlin Heidelberg, pp. 1–7.